JOURNAL OF SOLID STATE CHEMISTRY 77, 264–274 (1988)

Crystal Chemistry and Magnetic Behavior of Graphite Intercalation Compounds with Transition Metal Fluorides

S. FLANDROIS,*,[1] J. GRANNEC,† C. HAUW,‡ B. HUN,* L. LOZANO,†
AND A. TRESSAUD†

**Centre de Recherche Paul Pascal, †Laboratoire de Chimie du Solide du CNRS, and ‡Laboratoire de Cristallographie et de Physique Cristalline, Université de Bordeaux I, 33405 Talence Cedex, France*

Received February 12, 1988; in revised form June 22, 1988

Intercalation of RuF_5 and OsF_5 into graphite has been investigated using the vapor phase method. Stage 3 to stage 1 compounds were obtained depending on experimental conditions. The unit-cell constants of the intercalated layers were determined on Weissenberg patterns of a single crystal of $C_{20}RuF_{4.5}$ composition. A possible arrangement of $(RuF_4)_n$ chains containing ruthenium in octahedral coordination is proposed. A charge transfer of 0.5 electron per intercalated $RuF_{4.5}$ unit is deduced from the variation of C–C bond length. Structural phase transitions have been investigated on single crystals between 120 K and room temperature. The material shows a metallic behavior and a hysteresis phenomenon occurring around 130 K in the resistivity variation may result from an incommensurate $\rightleftharpoons$ commensurate transition. The magnetic behavior of Ru- and Os-intercalated salts is completely different from that of pure pentafluoride and corresponds to Ru(+IV) and Os(+V) species, respectively.

I. Introduction

Among graphite intercalation compounds (GIC) containing fluoride species in an appreciable amount, only a few examples are available which are based on transition metal fluorides. However, these materials could be of great interest in connection with high electrical conductivity (the highest conductivities have been obtained with SbF_5 and AsF_5 graphite compounds), low-dimensional magnetism (metal fluorides have various magnetic behaviors), and electrochemistry (they could give rise to rechargeable lithium batteries).

In the 3*d* transition series, TiF_4 yields third- or second-stage GIC, depending on the synthesis procedure (*1*, *2*), whereas very low rates of CuF_2 or FeF_3 have been intercalated into graphite, together with fluorine (*3*, *4*). Most of the studies have been devoted to hexafluorides of 4*d* and 5*d* transition series, such as MoF_6, TcF_6, OsF_6, IrF_6, PtF_6 (*5*, *6*). Intercalation may be obtained by exposing graphite to hexafluoride vapors. To our knowledge, only two transition metal pentafluorides have been successfully intercalated, namely NbF_5 and TaF_5 (*7*). In that case the presence of an oxidant like chlorine or fluorine gas is required for the intercalation to occur.

This paper deals with the reaction of 4*d* and 5*d* pentafluorides with graphite, and more especially of RuF_5 and OsF_5. Osmium

---

[1] Send correspondence to: S. Flandrois, Centre de Recherche Paul Pascal, Domaine Universitaire, 33405 Talence Cedex, France.

0022-4596/88 $3.00

fluoride has been previously intercalated as hexafluoride and no ruthenium fluoride GIC has been prepared up to now. These pentafluorides exhibit low melting points, and their structural and magnetic data have been previously investigated (*8–10*). Preliminary results have shown that the intercalation occurred at relatively low temperatures (*11*).

II. Experimental

1. Starting Materials

Various types of graphite have been used: highly oriented pyrolytic graphite (HOPG) from Union Carbide Company, flaky natural graphite (0.2 to 1 mm diameter), and powdered natural graphite (100 μm grain size) from Madagascar. Prior to any reaction, the graphite samples were purified from water absorption by heating at 150°C under vacuum.

Ruthenium and osmium pentafluorides were prepared by direct fluorination of the powdered metals. In a first step the metals were treated at 200°C under 4 to 5 bar fluorine pressure in a passivated nickel reactor (C) of the "fluorination line" shown in Fig. 1. The material condensed onto the cooled parts was then dropped to the bottom of the container. This step was carried out in a dry atmosphere, since Ru and Os pentafluorides are extremely sensitive to hydrolysis. A second treatment was performed at 100°C under a fluorine pressure of 1 bar. Crystalline powders of RuF_5 or OsF_5 were collected on the cooled upper part of the reactor. The melting temperatures of these two compounds are 86 and 70°C, respectively.

2. Synthesis of Metal Pentafluoride GICs

The synthesis of metal pentafluoride GICs was carried out in the same equipment. A mixture of graphite and MF_5 was heated under vacuum in a Ni reactor which had been previously passivated (container C in Fig. 1). The reaction temperatures were 120 and 90°C for M = Ru and Os, respectively. The reaction time was about 20 hr. The influence of the experiment duration has been tested up to 100 hr but no further weight uptake has been noted. The GICs were recovered after sublimation of

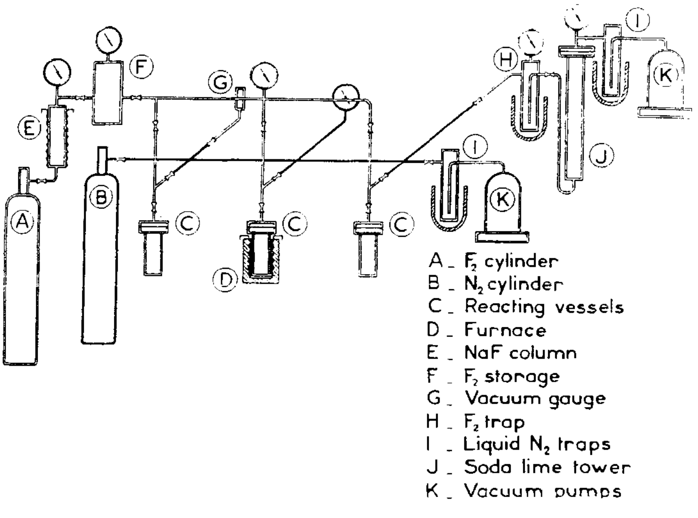

FIG. 1. Fluorination equipment.

the excess of pentafluoride by cooling the upper part of the reactor. These compounds were unstable in moist air and they were therefore handled in a dry atmosphere.

The influence of the type of pristine graphite has also been investigated: powdered graphite reacts more easily than large flakes or than HOPG. The most important intercalation rates (first stage compounds) have been obtained when the metal pentafluoride was in large excess relative to carbon, i.e., for ratios $MF_5/C \geq 5$.

3. *Elemental Analysis*

The gravimetric composition was obtained by weighing the material before and after intercalation. The weight uptake reached 300% in the case of RuF_5 and 280% in that of OsF_5. Assuming that the intercalated species has a MF_5 formula, the corresponding nominal compositions were close to "$C_{5.45}RuF_5$" and "$C_{8.4}OsF_5$" formulas for the highest intercalations.

The GICs were analyzed at Service Central d'Analyse du CNRS and in our laboratories. In the latter case a complete oxidation of the materials was carried out in a digestion bomb (Parr Instruments Co.) using sodium peroxide. The oxidized products were dissolved for spectrophotometric analysis. It should be noted that the F/Ru and F/Os ratios could not be obtained with great accuracy due to several experimental drawbacks:

—a short stability of the solutions in which a precipitation of "ruthenium black" often occurred,

—a possible formation of highly toxic osmium oxides,

—the presence of sodium which interfered in the atomic absorption results.

The F/Ru elemental ratio was also evaluated using a gravimetric method by oxidation of the compound in air and the formation of RuO_2. For the first stage compound obtained from the reaction of RuF_5 on powdered graphite this ratio is F/Ru = 4.5 ± 0.5 and the composition deduced from both elemental and gravimetric analyses is therefore $C_{5.2\pm0.5}RuF_{4.5\pm0.5}$. Concerning Os^- based materials, their compositions have been deduced from weight uptake only and the first stage compound corresponds to $C_{8.4}OsF_5$.

4. *Physical Characterizations*

Structural information was obtained using various X-ray data:

—powder diffraction patterns in order to determine the presence of pure or mixed stages, the repeat distances I_c along the c axis and the thickness of the intercalate,

—Weissenberg and Buerger photographs on single crystals at various temperatures between 77 and 300 K in order to characterize the sublattices of the intercalated species,

—an automatic diffractometer study to obtain accurate values of C–C bond lengths after intercalation.

Magnetic measurements were performed using a SQUID magnetometer (S.H.E. Corp.) in the 2–300 K temperature range with applied fields up to 6 T.

Electrical conductivities were obtained using a contactless method at Laboratoire de Chimie Minérale Appliquée, Université de Nancy, France, for Ru fluoride-GIC and at the Laboratory of Applied Solid State Chemistry, Kyoto University, Japan, for Os fluoride-GIC.

III. Structural Properties

1. *Ru Fluoride-GIC*

Powder diffraction data. Stage 1 compounds can be obtained with powdered graphite whereas larger flakes or HOPG lead generally to stages 2 and 3, and most often to a mixture of stages. The repeat distances I_c along the **c** axis have been evaluated to be 8.42 ± 0.05, 11.9 ± 0.1, 15.3 ± 0.1 Å, for stages 1, 2, and 3, respectively.

In the case of the reaction of RuF_5 in excess on powdered graphite, a stage 1 compound is obtained with a $C_{5.2}RuF_{4.5}$ formula. In this compound the intercalated layer has a thickness of $8.42 - 3.35 = 5.07 \pm 0.05$ Å. The salient feature of pure RuF_5 and OsF_5 is the presence of M_4F_{20} tetramers formed by four octahedra connected by corners (*9, 10*). The thickness of such units is about 5.8 ± 0.3 Å and a possible intercalation of ruthenium tetramers within the gallery may be therefore ruled out. The observed I_c value would better fit with RuF_6 octahedra with two faces parallel to the graphene planes: $(RuF_6)^{2-}$ and $(RuF_6)^-$ ions actually have a height of 4.97 and 4.93 Å, respectively. A similar assumption can be proposed for higher stage intercalations.

Single crystal data of $C_{20}RuF_{4.5}$ *at room temperature.* Weissenberg photographs on a single crystal of composition $C_{20}RuF_{4.5}$ (from natural graphite) have confirmed the value of I_c. However, we have noted the presence of a mixture of different stages and of a translational disorder which yields diffuse lines along the **c** axis of the reciprocal lattice. This latter point is often observed in GICs and indicates the absence of correlations between successive intercalated layers and probably even in the same layer (*12, 13*). A schematic diagram of a precession photograph of $C_{20}RuF_{4.5}$ is shown in Fig. 2a. Besides the hexagonal lattice of the graphitic layer, one can observe numerous reflections relative to the intercalated species. Most of these diffraction spots may be attributed to an oblique sublattice with a 7.8-Å edge and a 42° angle. This cell is not commensurate with that of graphite and may take three possible orientations related one to each other by a 60° rotation. The deviation angle between these two cells is 9° (Fig. 2c).

The ratio between the area of the intercalate cell and the area occupied by one carbon atom is 15.5, a value which may lead to the following compositions for a first-stage compound: $C_{15.5}RuF_x$, $C_{7.8}RuF_x$, and $C_{5.1}RuF_x$ depending on the number of Ru atoms located in the cell: 1, 2, or 3 namely. The third proposal which is associated with the presence of three Ru atoms within the intercalate cell better fits the $C_{5.2}RuF_{4.5}$ formula which had been deduced from elemental and gravimetric analyses. If we assume that the Ru atoms are located at the center of octahedral vacancies of an hexagonal packing of fluorine atoms, a possible arrangement can be proposed as shown in Fig. 2d. In this model, RuF_6 octahedra would form parallel chains with two different Ru–Ru distances of 2.6 and 3 Å, which would involve a slight distortion of the octahedra. On the other hand, there would be only 12 fluorine atoms per cell, i.e., F/Ru = 4, a value which is lower than that deduced from analyses. This discrepancy could be attributable to an incomplete filling of the galleries and to a subsequent island structure of the intercalated species, leading to an excess of fluorine atoms.

In addition, these proposals do not take into account the presence of weaker diffraction spots which may correspond to other types of intercalated species such as $(RuF_6)^{2-}$.

Charge transfer. It has been previously shown that the C–C bond length in the graphene plane changes by intercalation and that the variation can be correlated with the amount of charge transfer (*13*). For electron donor-GICs the C–C bond length increases, whereas for electron acceptor-GICs a contraction of these bonds is observed due to the involvement of π antibonding orbitals. Several theoretical studies have been devoted to this problem (*14*) and an empirical relationship between charge transfer and C–C bond length has been proposed for acceptor compounds, based on the chlorine excess observed in

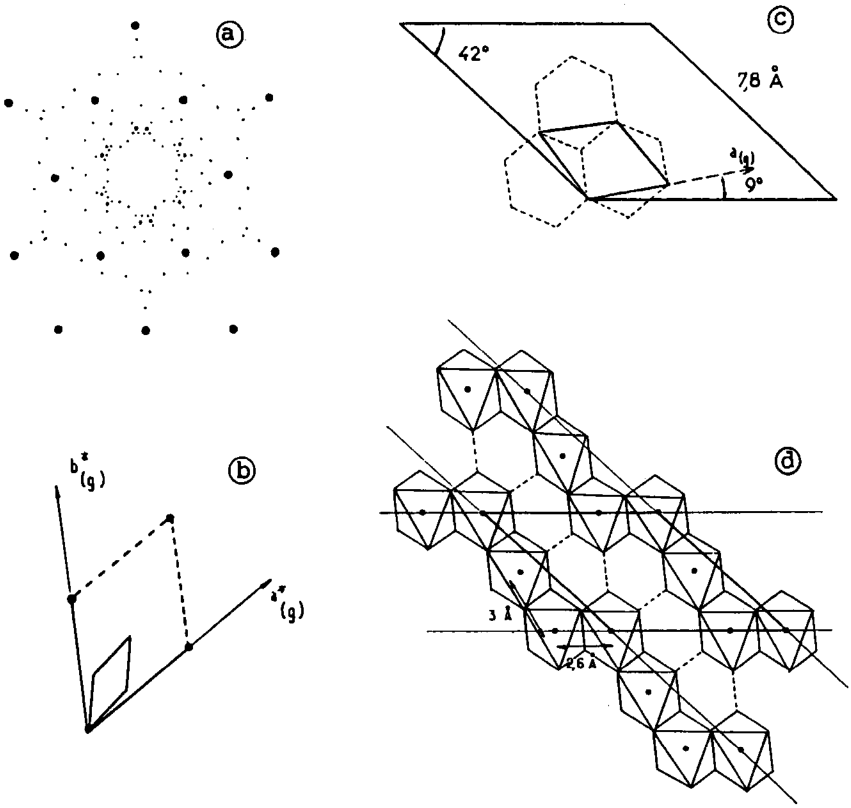

FIG. 2. Schematic diagram of precession patterns of $C_{20}RuF_{4.5}$ at 300 K (a). Relationships between the sublattices of the intercalated species and that of graphitic layers in the reciprocal lattice (b), and in the direct lattice (c). Possible arrangement of $(RuF_4)_n$ chains at 300 K (d).

metal chloride-GICs (*15*). This relationship is shown in Fig. 3 together with the theoretical results (dashed lines) from Pietronero and Strässler (PS) and Chan *et al.* (CKHE).

The accurate determination of the position of (110) reflection of the graphitic sublattice has been carried out on a single crystal with $C_{20}RuF_{4.5}$ composition. The observed C–C bond length $d_{c-c} = 1.4191(4)$ Å is actually contracted relative to that of pristine graphite: $d_{c-c} = 1.4209(1)$ Å. From the relationship given in Fig. 3, the value of d_{c-c} for $C_{20}RuF_{4.5}$ corresponds to a charge transfer of 0.025 electron per C atom, i.e., 0.5 electron per intercalated $RuF_{4.5}$. This result can be compared to those proposed for AsF_5-GIC which ranged from 0.2 to 0.5 electron per intercalated molecule (*16*).

Structural phase transitions. The occurrence of a phase transition has been detected during the electrical conductivity study at about 130 K (see Section IV). Precession photographs have therefore been taken on a single crystal with $C_{20}RuF_{4.5}$ composition above and below this temperature in order to clarify whether the transition could be ascribed to structural changes.

At 160 K, most of the diffraction spots corresponding to the intercalate can be indexed in a new cell with an hexagonal symmetry. This sublattice which has a 6.9-Å

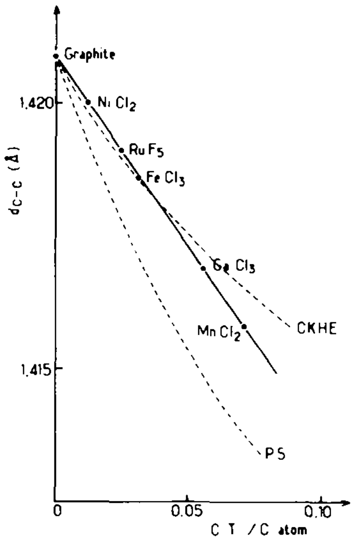

FIG. 3. Charge transfer per carbon atom as a function of C–C bond length. Full line: empirical relationship from Ref. (*15*), based on the data points obtained for several metal chloride GICs. Dashed lines: theoretical calculations (*14*) from Pietronero and Strässler (PS) and Chan *et al.* (CKHE).

edge is rotated by 30° relative to the graphite direction (Fig. 4c). Its area is similar to that observed at room temperature. The two networks are incommensurate. The additional weak reflections observed at 300 K are still present but they are much weaker. A gliding of the chains could occur which would take into account the characteristics of this new sublattice.

Another transition occurs at lower temperatures. In the precession photographs taken at 120 K, a new intercalate sublattice appears, whose unit cell is a parallelogram of 7.4 Å × 5.6 Å edges and a 50° angle (Fig. 4c). The two sublattices (intercalate and graphene) are now commensurate. The remanence at 120 K of the diffraction spots observed at 160 K may be ascribed to an incomplete transition process, since the hysteresis phenomenon has not completely vanished at that temperature (see Fig. 5).

These structural evolutions have been shown to be reversible.

2. *Os Fluoride-GIC*

When the intercalation of OsF_5 in powdered graphite is carried out in the presence of a large excess of pentafluoride, a stage 1 compound is obtained with a nominal composition $C_{8.4}OsF_5$. The identity period along the **c** axis, $I_c = 8.3$ Å, corresponds to intercalated layers of thickness: $8.3 - 3.35 = 4.95 + 0.05$ Å. Here again the presence of Os_4F_{20} tetramers can be ruled out. The intercalated species should be OsF_6 octahedra with two faces parallel to the graphite planes, in good agreement with the calculated height of $(OsF_6)^-$ octahedra: $h = 4.97$ Å, with $r(Os^V) = 0.67$ Å (*16*).

The precession photographs of the stage 1 compound show, besides the graphite spots, a diffuse ring whose *d*-spacing values range from 4.8 to 5.9 Å. This type of reflection is characteristic of a disordered two-dimensional phase.

IV. In-Plane Electrical Resistivity

The in-plane electrical resistivities ρ_a have been measured on HOPG samples showing X-ray diffraction lines characteristic of a stage 3 compound.

1. *Ru Fluoride-GIC*

At room temperature, the resistivity value is twice lower than that of pristine graphite. However, a small weight uptake (~30%) [compared with the theoretical value of 100% for a pure stage 3] and a still high value of the resistivity might be due to an intercalation limited to the external part of the sample. The thermal dependence of the resistivity is given in Fig. 5 and is consistent with a metallic behavior generally observed for acceptor-GICs (*17*). In addition, a transition in the resistivity occurs about 130 K, which is associated with a hysteresis. This type of phenomenon, which suggests a first-order phase transition, already has been observed in alkali

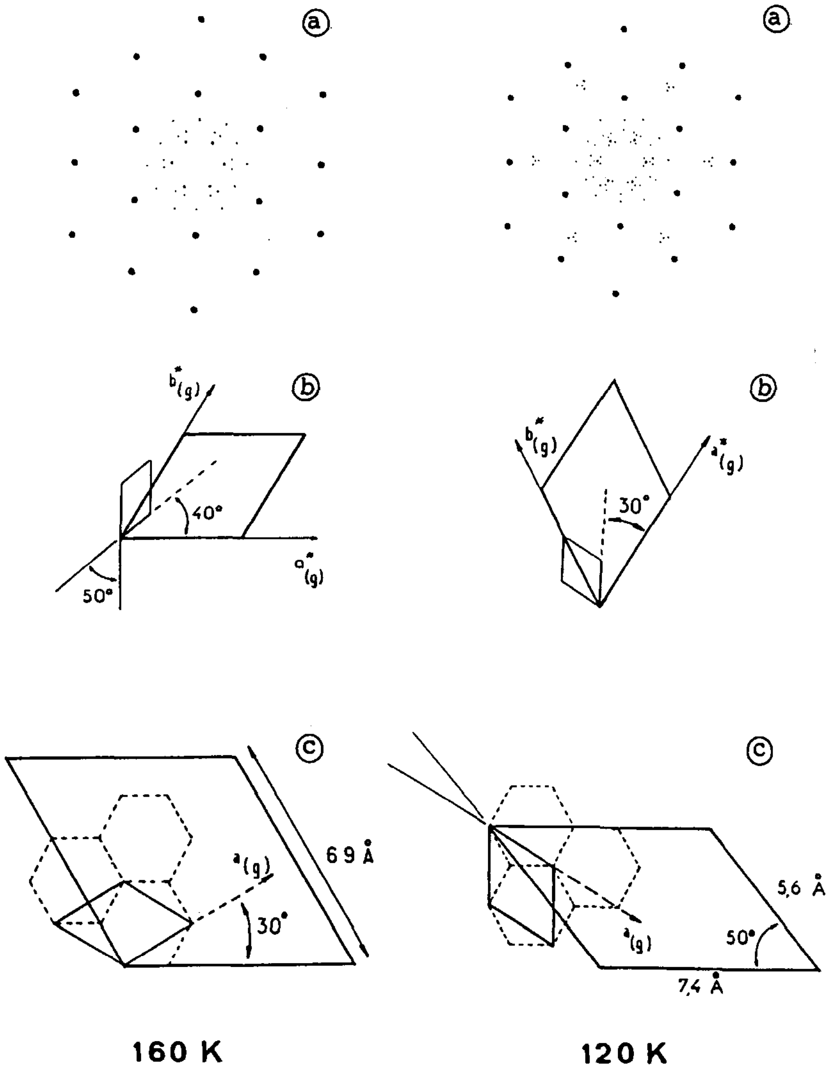

FIG. 4. Schematic diagrams of precession patterns of $C_{20}RuF_{4.5}$ at 160 and 120 K (a). Relationships between the sublattices of the intercalate and the graphene layers in the reciprocal lattice (b), and in the direct one (c).

metal-GICs and has been correlated to an ordering of alkaline atoms in the intercalate layers (*18, 19*). The decrease of the resistivity around 130 K could result from the incommensurate $\rightleftharpoons$ commensurate transition observed by X-ray diffraction.

2. *Os Fluoride-GIC*

The resistivity measurements have been performed on ill-defined stage 3 material of $C_{30}OsF_5$ composition, at room temperature only. The intercalation of OsF_5 induces a decrease in the resistivity about four times relative to that of pristine graphite.

The high conductivities observed at room temperature ($\sigma \approx 0.2 \times 10^5$ Scm^{-1}) are comparable with those of other GICs based on $FeCl_3$, $CuCl_2$, ... However, their values do not reach those claimed for AsF_5- or SbF_5-based GIC ($\sigma \approx 5 \times 10^5$ Scm^{-1}).

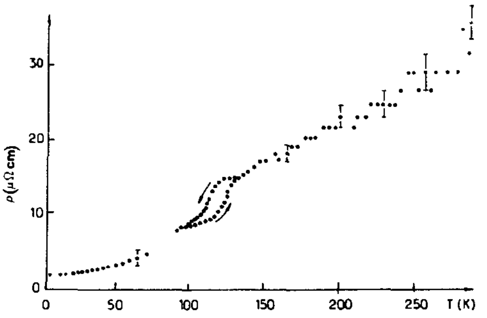

FIG. 5. Temperature dependence of electrical resistivity of a stage 3 $C_xRuF_{4.5}$ compound.

V. Magnetic Properties

1. *Tetrameric-type Magnetism of Pristine RuF_5*

The temperature dependence of the magnetic susceptibility of pristine RuF_5 at high temperature obeys the Curie–Weiss law with $\theta_p = -52$ K and $C = 1.93$ emu K mole^{-1} (*10*). A maximum of susceptibility is observed around 40 K. Over a large temperature range, the temperature dependence of χ_m has been explained in terms of isolated tetrameric Ru_4F_{20} clusters (Fig. 6a). Theoretical calculations based on antiferromagnetic interactions between nearest Ru(+V) neighbors of identical spin $S = 3/2$ yield an intracluster exchange constant $J/k \approx -8$ K (*10, 21*). At low temperatures ($T \lesssim 40$ K) the discrepancy observed between the experimental points and the theoretical curve is due to the occurrence of 3D magnetic interactions. Below the ordering temperature, $T_N = 5$ K, a strong dependence of the magnetization vs the applied field has been observed (Fig. 6b).

2. *Magnetic Behavior of $C_{5.2}RuF_{4.5}$*

The temperature dependence of the magnetic susceptibility of the stage 1 compound $C_{5.2}RuF_{4.5}$ is completely different from that of the pure pentafluoride as shown in Fig. 7. Over most of the temperature range, a Curie–Weiss behavior is observed with $\theta_p = -47$ K. This value, which is similar to that of pure pentafluoride, confirms the presence of strong antiferromagnetic interactions between Ru atoms. However, no minimum is observed in the $\chi^{-1} = f(T)$ curve around 40 K, nor is there an influence

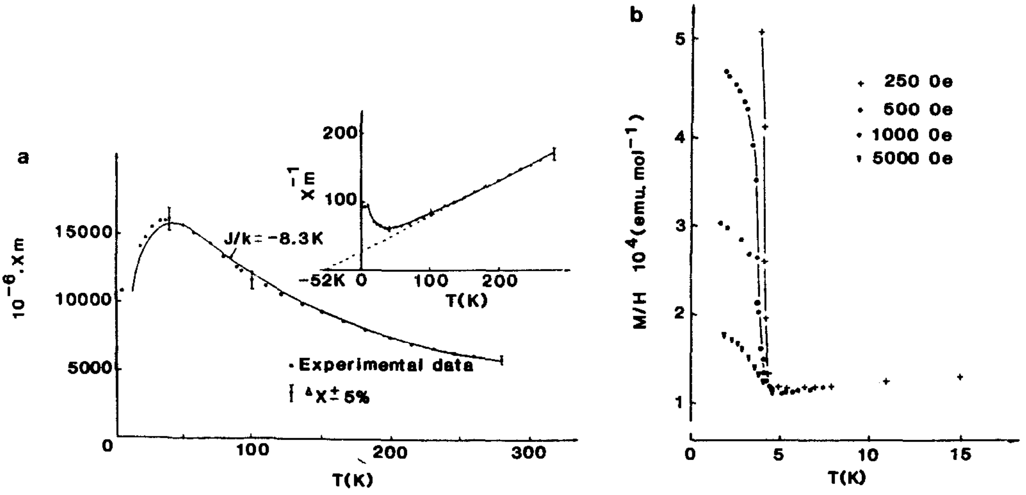

FIG. 6. Thermal dependence of the magnetic susceptibility of pure RuF_5 (from (7)) (a); temperature dependence of the ratio M/H RuF_5 (b).

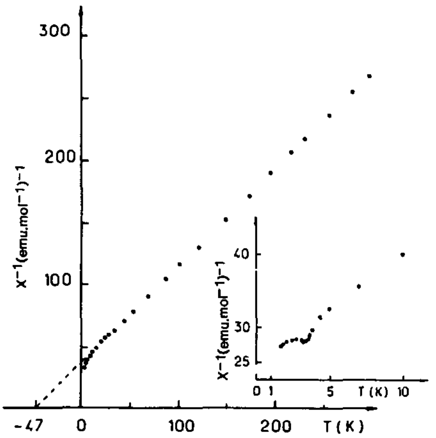

FIG. 7. Temperature dependence of the reciprocal susceptibility of $C_{5.2}RuF_{4.5}$.

of the structural transition at 130 K. The field dependence of the magnetization remains linear down to 2 K, at least for $H \leq 10$ kOe. An anomaly has been detected at 3 K, which could correspond to a 3D ordering.

The Curie constant is $C_m = 1.23 \pm 0.06$ emu K mole^{-1} for one mole of $C_{5.2}RuF_{4.5}$ ($M_{eff} = 3.14 \pm 0.09$ μ_B). This value is close to that calculated for Ru(+IV) [$M_{eff} = 2.9$ μ_B with $S = 1$ and $g = 2$ (*18*, *19*)], whereas that expected for Ru(+V) is $M_{eff} = 3.9$ μ_B with $S = 3/2$ and $g = 2$ (*10*, *21*).

The presence in the stage 1 compound of mostly tetravalent ruthenium is in good agreement with a charge transfer of 0.5 electron per $RuF_{4.5}$ unit. For crystallographic reasons the assumption of $(RuF_4)_n$ neutral chains of edge-shared octahedra as the main component of intercalated species has been proposed above (see Fig. 2). The excess of fluorine atoms may be attributed either to the presence of $(RuF_6)^{2-}$ isolated octahedra or to $(Ru_nF_{4n+2})^{2-}$ segments of chains with $n \geq 2$. However, the latter assumption, which had been already proposed for metal chloride GIC (*12*), cannot fit the number of Ru atoms (i.e., 3) present in the cell of the intercalate sublattice shown in Fig. 2. The presence in the compound of 25% of $(RuF_6)^{2-}$ isolated octahedra together with 75% of $(RuF_4)_n$ chains would be therefore a possible solution to achieve the $RuF_{4.5}$ stoichiometry and to take into account analytical, magnetic, and crystallographic data.

3. *Magnetic Behavior of $C_{8.4}OsF_5$*

The temperature dependence of the susceptibility for the stage 1 compound $C_{8.4}OsF_5$ is similar to that of the Ru homologue as shown in Fig. 8a. In most of the temperature range it obeys a Curie–Weiss relation with $\theta_p = -57$ K, indicating strong antiferromagnetic interactions between Os atoms. No maximum in susceptibility is observed around 60 K, implying the absence of tetrameric Os_4F_{20} units.

Assuming a F/Os ratio of 5, the molar Curie constant is $C_m = 1.14$ emu K mole^{-1}, which corresponds to an effective moment $M_{eff} = 3.02$ μ_B. This value is close to that generally found for Os(+V) [$M_{eff} = 3.2$ μ_B] (*24*, *25*). It should be noted that a different choice of the F/Os ratio would not notably alter the experimental value of M_{eff}, due to the important atomic weight of osmium: even assuming a F/Os ratio of 4, the deduced effective moment is $M_{eff} = 2.94$ μ_B, whereas the Os(+IV) moment is expected to be much lower: $M_{eff} \approx 1.5 \pm 0.2$ μ_B (*22*). It seems therefore reasonable to anticipate that osmium is present in its pentavalent oxidation state in the intercalated species. At low temperatures, the variation of the magnetization with the applied field is linear, at least for $H \leq 2$ kOe; no anomalous susceptibility behavior has been noted above 2 K. For higher H values a saturation mechanism occurs (Fig. 8b).

The above results can be compared with those obtained by Bartlett *et al.* (*5*) and Vaknin *et al.* (*24*) for the intercalation of gaseous OsF_6 in HOPG: the intercalated species were $(OsF_6)^-$ groups and the magnetic moment was equal to 3.2 μ_B. The

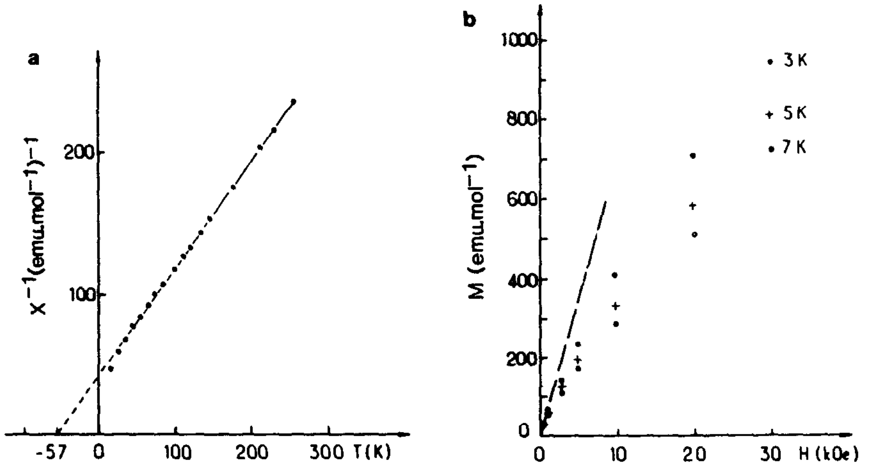

FIG. 8. Temperature dependence of the reciprocal susceptibility of $C_{8.4}OsF_5$ (a). Field dependence of the magnetization of $C_{8.4}OsF_5$ at low temperatures (b).

magnetic behavior at low temperature was anisotropic and depended on the direction of the applied field relative to the graphite planes. They could not detect any magnetic ordering either. Our results are consistent with those proposed by these authors. Pentavalent osmium would be located in octahedra exhibiting two faces parallel to the graphene layers. Very weak magnetic interactions would occur between these species since no peculiar feature is noticeable down to 2 K.

VI. On the Mechanism of Intercalation of RuF_5 and OsF_5

The present study shows the complexity of the intercalation of metal fluorides in comparison with other acceptor compounds such as metal chlorides. Whereas the intercalated chloride species are generally of only one kind and have a structure close to that of the free chlorides (with the same oxidation state of the metal), the layers of intercalated fluorides can be made up of several species whose arrangement does not reproduce the structure of the free fluorides. The reduction of ruthenium from Ru(+V) to Ru(+IV) occurs during the intercalation of RuF_5, with two kinds of intercalated species: ionic RuF_6^{2-} (isolated ions) and neutral RuF_4 (chain-like structure). Similarly, the tetrameric structure of pristine OsF_5 does not exist after intercalation. In this case, however, the oxidation state Os(+V) is maintained. This result has to be compared with those obtained by Selig and co-workers (*6*, *24*) for the intercalation of osmium hexafluoride, where Os(+VI) is reduced to Os(+V); the presence of OsF_6^- intercalated species was claimed. Many similarities seem to exist between compounds prepared from OsF_6 and OsF_5, for the magnetic behavior as well as for the structure of the intercalated layers, which is liquid like at room temperature (*26*). It strongly suggests the presence of similar intercalated species. For these species to be OsF_6^- ions, the following reaction should occur,

$$2\,OsF_5 + e^- \rightarrow OsF_4 + OsF_6^-$$

with only intercalation of OsF_6^-. However, the simultaneous intercalation of an appreciable amount of neutral OsF_5 cannot be ruled out. Clearly, considerably more study is needed before the intercalation mechanism of metal fluorides can be fully understood.

Acknowledgments

We are grateful to E. McRae, J. F. Mareche, and H. Touhara for conductivity measurements.

References

1. E. Buscarlet, P. Touzain, and L. Bonnetain, *Carbon* **14,** 75 (1976).
2. S. Flandrois, B. Hun, J. Grannec, A. Tressaud, and C. Hauw, *Synth. Met.* **23,** 435 (1981).
3. T. Nakajima, M. Kawaguchi, and N. Watanabe, *Carbon* **20,** 287 (1982).
4. M. Kawaguchi, Thesis, Kyoto University (1984).
5. N. Bartlett, E. M. McCarron, B. W. McQuillan, and T. E. Thompson, *Synth. Met.* **1,** 221 (1979/1980).
6. H. Selig, D. Vaknin, D. Davidov, and Y. Yeshurun, *J. Chem. Soc. Chem. Commun.*, 1189 (1985); D. Vaknin, D. Davidov, V. Zevin, and Y. Yeshurun, *Phys. Rev. B* **35,** 6423 (1985); I. Bleish, D. Vaknin, D. Davidov, H. Selig, and J. Kjems, *Synth. Met.* **23,** 351 (1988).
7. J. Melin and A. Herold, *C.R. Acad. Sci. C* **280,** 641 (1975); D. Ravaine, J. Boyce, A. Hamwi, and P. Touzain, *Synth. Met.* **2,** 249 (1980); A. Hamwi, S. Mouras, D. Djurado, and J. C. Cousseins, *in* "Proceedings of the Carbon 86 Conference, Baden-Baden, 1986," p. 454.
8. S. J. Mitchell and J. H. Holloway, *J. Chem. Soc.*, 2789 (1971).
9. B. K. Morrell, A. Zalkin, A. Tressaud, and N. Barlett, *Inorg. Chem.* **12,** 2640 (1973).
10. J. Darriet, L. Lozano, and A. Tressaud, *Solid State Commun.* **32,** 493 (1979).
11. A. Tressaud, J. Grannec, B. Hun, S. Flandrois, and C. Hauw, *Synth. Met.* **18,** 558 (1987).
12. J. M. Masson, Thesis, University Bordeaux I (1979).
13. S. Flandrois, J. M. Masson, J. C. Rouillon, J. Gaultier, and C. Hauw, *Synth. Met.* **3,** 1 (1981).
14. L. Pietronero and S. Strässler, *Phys. Rev. Lett.* **47,** 593 (1981); M. Kertesz, *Mol. Cryst. Liq. Cryst.* **125,** 103 (1983); C. T. Chan, W. A. Kamitakahara, K. M. Ho, and P. C. Eklund, *Phys. Rev. Lett.* **58,** 1528 (1987).
15. F. Baron, S. Flandrois, C. Hauw, and J. Gaultier, *Solid State Commun.* **42,** 759 (1982).
16. T. E. Thompson, E. M. McCarron, and N. Bartlett, *Synth. Met.* **3,** 255 (1981).
17. R. D. Shannon, *Acta Crystallogr. A* **32,** 751 (1976).
18. S. Flandrois and J. Herran, *Synth. Met.* **14,** 103 (1986).
19. K. Phan, C. D. Fuerst, and J. E. Fisher, *Solid State Commun.* **32,** 493 (1979).
20. F. Beck, H. Krohn, and W. Kaiser, *J. Appl. Electrochem.* **12,** 505 (1982).
21. J. Darriet, J. L. Soubeyroux, H. Touhara, A. Tressaud, and P. Hagenmuller, *Mat. Res. Bull.* **17,** 315 (1982).
22. A. Earnshaw, B. N. Figgis, J. Lewis, and R. D. Peacock, *J. Chem. Soc.*, 3132 (1961).
23. J. H. Holloway and R. D. Peacock, *J. Chem. Soc.*, 3892 (1963).
24. D. Vaknin, D. Davidov, H. Selig, V. Zevin, I. Felner, and Y. Yeshurun, *Phys. Rev. B* **31,** 3212 (1985).
25. B. N. Figgis, J. Lewis, and F. E. Mabbs, *J. Chem. Soc.*, 3138 (1961).
26. J. K. Kjems, Y. Yeshurun, D. Vaknin, D. Davidov, and H. Selig, *Phys. Rev. B* **36,** 6981 (1987).